molecular pharmaceutics

Brief Article

pubs.acs.org/molecularpharmaceutics

Analysis of Cancer-Targeting Alkylphosphocholine Analogue Permeability Characteristics Using a Human Induced Pluripotent Stem Cell Blood–Brain Barrier Model

Paul A. Clark,[†] Abraham J. Al-Ahmad,[‡] Tongcheng Qian,[§] Ray R. Zhang,[†,∥] Hannah K. Wilson,[§] Jamey P. Weichert,[∥,⊥] Sean P. Palecek,[§] John S. Kuo,[*,†] and Eric V. Shusta[*,§]

[†]Departments of Neurological Surgery, [§]Chemical and Biological Engineering, and [∥]Radiology, University of Wisconsin—Madison, Madison, Wisconsin 53792, United States

[⊥]Cellectar Biosciences, Madison, Wisconsin 53716, United States

[‡]Department of Pharmaceutical Sciences, Texas Tech University Health Sciences Center—School of Pharmacy, Amarillo, Texas 79106, United States

ABSTRACT: Cancer-targeting alkylphosphocholine (APC) analogues are being clinically developed for diagnostic imaging, intraoperative visualization, and therapeutic applications. These APC analogues derived from chemically synthesized phospholipid ethers were identified and optimized for cancer-targeting specificity using extensive structure–activity studies. While they strongly label human brain cancers associated with disrupted blood–brain barriers (BBB), APC permeability across intact BBB remains unknown. Three of our APC analogues, CLR1404 (PET radiotracer), CLR1501 (green fluorescence), and CLR1502 (near-infrared fluorescence), were tested for permeability across a BBB model composed of human induced pluripotent stem cell-derived brain microvascular endothelial cells (iPSC-derived BMECs). This in vitro BBB system has reproducibly consistent high barrier integrity marked by high transendothelial electrical resistance (TEER > 1500 Ω-cm^2) and functional expression of drug efflux transporters. The radioiodinated and fluorescent APC analogues demonstrated fairly low permeability across the iPSC-BMEC (35 ± 5.7 (CLR1404), 54 ± 3.2 (CLR1501), and 26 ± 4.9 (CLR1502) × 10^{-5} cm/min) compared with BBB-impermeable sucrose (13 ± 2.5) and BBB-permeable diazepam (170 ± 29). Only the fluorescent APC analogues (CLR1501, CLR1502) underwent BCRP and MRP polarized drug efflux transport in the brain-to-blood direction of the BBB model, and this efflux can be specifically blocked with pharmacological inhibition. None of the tested APC analogues appeared to undergo substantial P-gp transport. Limited permeability of the APC analogues across an intact BBB into normal brain likely contributes to the high tumor to background ratios observed in initial human trials. Moreover, addition of fluorescent moieties to APCs resulted in greater BMEC efflux via MRP and BCRP, and may affect fluorescence-guided applications. Overall, the characterization of APC analogue permeability across human BBB is significant for advancing future brain tumor-targeted applications of these agents.

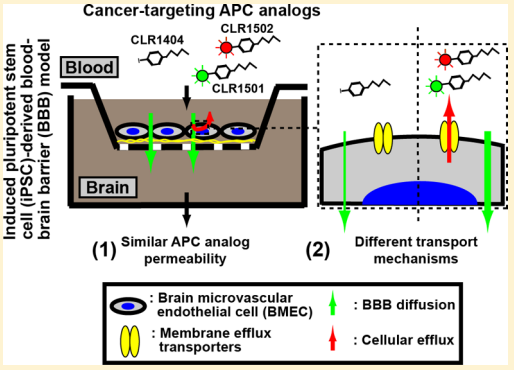

KEYWORDS: *alkylphosphocholine analogues, blood–brain barrier, brain microvascular endothelial cells, induced pluripotent stem cells*

INTRODUCTION

Efficient treatment for central nervous system (CNS) tumors is a large unmet clinical need. Approximately 25,000 new primary malignant brain tumors are annually diagnosed in the United States, accounting for 1.4% of all cancer-related deaths and the second leading cause of death in pediatric cancers.[1,2] Glioblastoma (GBM) is the most frequently diagnosed primary adult brain tumor that confers a median survival of less than two years despite maximal surgery, temozolomide chemotherapy, and radiation.[3] Furthermore, brain metastases from other cancer types such as melanoma, breast, and lung are approximately ten times more prevalent than primary CNS tumors in adults, and often herald advanced cancer stages due to limited effective treatments.[4] Chemotherapeutic delivery to brain neoplasms is hampered by the presence of the blood–brain barrier (BBB), formed by specialized brain microvascular endothelial cells (BMECs) and surrounded by other cells of the neurovascular unit including astrocytes, pericytes, and neurons.[5,6] At the BBB, BMECs incorporating specific tight junction proteins form a "tight" barrier defined by high transendothelial electrical resistance (TEER)[5,6] and low paracellular permeability to water and hydrophilic solutes. Additionally, the physical barrier function is augmented by the

Received: May 18, 2016
Revised: July 12, 2016
Accepted: July 15, 2016
Published: July 15, 2016

DOI: 10.1021/acs.molpharmaceut.6b00441
Mol. Pharmaceutics 2016, 13, 3341–3349

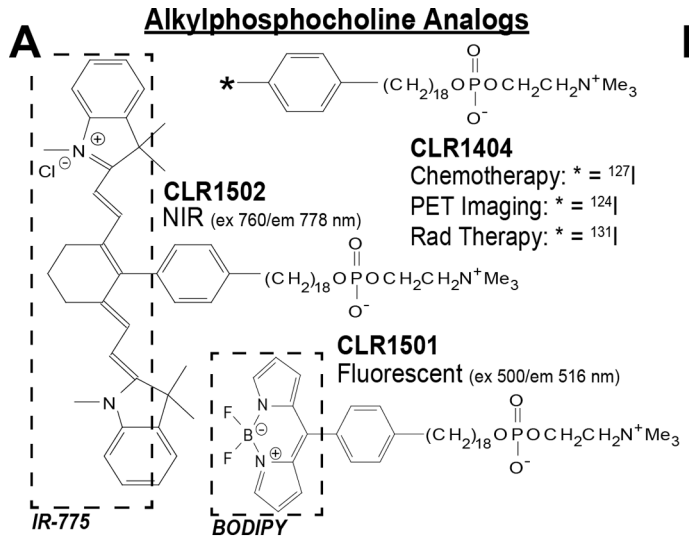

B

Compound	MW	cLogD	LogD (pH 7.4)
Diazepam	284.7	2.63	2.91[a]
Sucrose	342.3	-2.63	-3.48[a]
CLR1404	637.6	4.10	2.07±0.06
CLR1501	701.7	3.90	4.59±0.11
CLR1502	994.8	6.06	4.66±0.54

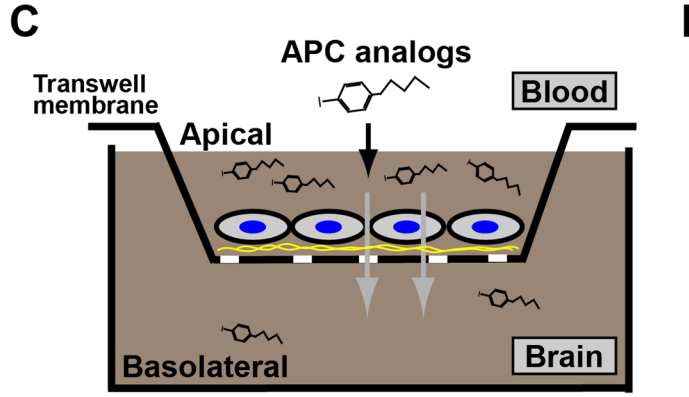

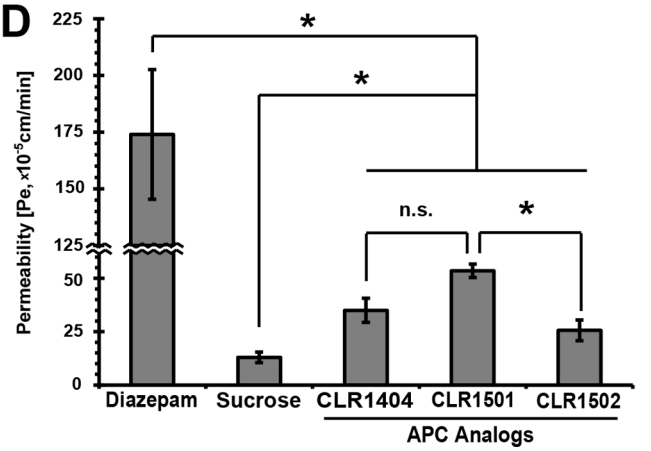

Figure 1. Biochemical properties and permeability of APC analogues across the iPSC-BBB Transwell system. (A) APC analogue chemical structures. (B) APC analogue octanol/water distribution coefficients (LogD), both calculated (cLogD) and experimental (LogD pH 7.4). [a]From ref 32. (C) Experimental setup to determine APC analogue in vitro BBB permeability (Pe) values. (D) APC analogue permeability of analogues compared with impermeable sucrose and highly permeable diazepam. (mean ± SE, $n \geq 3$ independent BMEC differentiation replicates, $^*p < 0.05$ or n.s. = not significant by ANOVA followed by post hoc Games−Howell tests).

presence of an active functional barrier due to multiple types of drug efflux pumps including breast cancer resistance protein (BCRP), multidrug resistance proteins (MRPs), and P-glycoprotein (P-gp) at the BMEC interface that limit diffusion of small lipophilic molecules into the CNS.[5,7,8]

Historically, the blood−brain tumor vasculature is described as "leaky" due to immature or disrupted BBB vasculature.[9−13] However, recent studies demonstrated intra- and intertumoral heterogeneity of BBB properties both in primary gliomas[13] and in metastases,[11] with different tumor regions exhibiting variable and sometimes highly restricted drug permeability.[13−16] Additionally, gliomas notoriously infiltrate normal brain parenchyma with intact BBB, making complete surgical resection very difficult and highlighting the need for more effective chemotherapeutic agents or delivery approaches that cross intact BBB.[13]

Cancer-targeting alkylphosphocholine (APC) analogues were recently described as tumor-specific labels for a broad range of cancer types including gliomas and brain metastases in cultured cell lines, preclinical models, and human cancer patients.[17,18] The observation that naturally occurring phospholipid ethers (PLEs) selectively accumulate in human cancer cells compared to normal tissue[19−21] prompted our group to examine structural activity relationships for radioiodinated aryl PLEs and a subset of APC derivatives to determine how their molecular structures affected tumor retention. From these studies, we found that the glycerol backbone was not required for tumor avidity in glycerol-derived PLE analogues, the alkyl chain must contain >11 methylene groups, and the position of iodine on the phenyl ring did not influence tumor uptake or specificity.[22−25] Ultimately, the APC molecular backbone named CLR1404 [18-(*p*-iodophenyl)octadecylphosphocholine] (Figure 1A) was identified as the best cancer-targeting APC analogue exhibiting both tumor-specific uptake and long-term retention. CLR1404 can be labeled with iodine radioisotopes for positron emission tomography (PET) imaging (^{124}I isotope) or radiotherapy (^{131}I or ^{125}I isotopes).[17] For this APC analogue, the iodine can also be replaced with fluorescent moieties (green fluorescent CLR1501 or near-infrared CLR1502) to yield similar tumor selectivity and retention, enabling potential intraoperative applications to improve tumor cell visualization and surgical resection.[18] All APC analogues exhibit particularly high tumor to normal brain ratios in vivo,[17,18] which is promising for brain tumor applications. However, BBB permeability properties of APC analogues are currently unknown.

DOI: 10.1021/acs.molpharmaceut.6b00441
Mol. Pharmaceutics 2016, 13, 3341−3349

In the current study, we used our recently described human induced pluripotent stem cell (iPSC) derived BMECs as an in vitro BBB model[26,27] to analyze and characterize the BBB permeability profiles of our APC analogues. The iPSC-derived BMECs exhibit well-developed BBB-BMEC tight junctions and a correspondingly high TEER with functionally polarized drug efflux transporters. Together, these properties have yielded in vitro permeability measurements for a cohort of small molecules that correlate to in vivo observations.[26,27] Permeability measurements with the APC analogues indicated a similar intermediate permeability across the in vitro BBB for all compounds, whereas efflux transporter activity was only observed for fluorescent APC analogues. These results suggest that limited BBB permeability of APC analogues may contribute to low APC uptake and retention in the normal brain parenchyma observed clinically, and that moieties added to the APC backbone can significantly affect BBB permeability.

MATERIALS AND METHODS

Chemicals. The APC analogues CLR1404, CLR1501, and CLR1502 were provided by Cellectar Biosciences, Inc. (Madison, WI, USA). These APC analogues consist of a cancer-targeting alkylphosphocholine scaffold with an attached cancer imaging, visualization, or therapeutic moiety (refs 17, 18, 25, and 28 and Figure 1): iodine isotopes for CLR1404; 4,4-difluoro-4-bora-3a,4a-diaza-*s*-indacene (i.e., BODIPY, green fluorescence) for CLR1501; and 2-[2-[2-chloro-3-[2-(1,3-dihydro-1,3,3-trimethyl-2*H*-indol-2-ylidene)ethylidene]-1-cyclohexen-1-yl]ethenyl]-1,3,3-trimethyl-3*H*-indolium chloride (i.e., IR-775, near-infrared fluorescence) for CLR1502. Pharmacological cellular efflux transporter inhibitors were purchased: PSC833 and Ko143 from Tocris Biosciences, and MK571 from Sigma-Aldrich (St. Louis, MO, USA). [^{14}C]-Sucrose and [^{3}H]-diazepam were purchased from American Radiolabeled Chemicals (St. Louis, MO, USA).

LogD Determination. For APC analogues CLR1404 (MW = 637.6 g/mol), CLR1501 (MW = 701.7 g/mol), and CLR1502 (MW = 994.8 g/mol), the SMILES sequences were determined using ChemDraw Pro 13.0 (PerkinElmer, Waltham, MA), and calculated LogD (cLogD) was calculated using the ALOGPs 2.1 algorithm.[29,30] Experimental LogD (pH 7.4) values were obtained by adding ^{124}I-CLR1404, CLR1501, and CLR1502 to octanol followed by equilibration overnight. Equal volumes of buffer (pH 7.4) were added, and the mixture was rotated at room temperature shielded from light for 48 h. The octanol and water phases were separated and then analyzed using the gamma counter (Wizard2 Automatic Gamma Counter, PerkinElmer, Waltham, MA) for ^{124}I-CLR1404 or Safire II (Tecan Group Ltd., Männedorf, Switzerland) for CLR1501 and CLR1502 to determine relative concentrations. Finally, the octanol:water partition coefficients were calculated.[31] LogD values for diazepam and sucrose were obtained from the literature.[32]

Differentiation of iPSC into BMEC. BMECs were differentiated from iPSCs following protocols previously established by our group.[26,27] IMR90-c4 iPSC cell line[33] was purchased from WiCell (Madison, WI) and passaged on 6-well tissue culture plates (Corning, Corning, NY) coated with 84 μg/mL of growth-factor reduced Matrigel (BD Biosciences) and grown in mTeSR1 (Stem Cell Technologies, Vancouver, BC). Cells were fed on a daily basis. After 3−4 days in mTeSR medium, cells were switched to a unconditioned medium (UM): 50:50 Dulbecco's modified Eagle medium: F12 (Gibco, Life Technologies, Carlsbad, CA), 15 mM HEPES (Sigma-Aldrich, St Louis, MO), 20% knockout serum replacement (Life Technologies), 1% nonessential amino acids (Life Technologies), 0.5 mM GlutaMax (Life Technologies), and 0.1 mM β-mercaptoethanol (Sigma-Aldrich). Cell medium was changed daily for 6 consecutive days. The BMEC population was further enriched by replacing the incubation medium with endothelial cell (EC) medium: human endothelial cell serum-free medium (Gibco), 20 ng/mL basic fibroblast growth factor (bFGF, R&D Systems, Minneapolis, MN), 1% platelet-poor derived bovine serum (PDS, Biotechnologies Inc., Boston, MA), and 10 μM retinoic acid (RA) for 48 h. Following endothelial cell enrichment, cells were dissociated using Accutase (Stempro, Life Technologies) for 30 min and seeded onto Transwell polycarbonate inserts (1.12 cm^2 surface area) coated with 0.4 mg/mL human collagen from human placenta (Sigma) and 0.1 mg/mL bovine fibronectin (Sigma). After allowing 24 h attachment, medium was removed from the inset and replaced with EC medium without bFGF and RA. Experiments were carried out 48 h after plating Transwell monolayers.

Differentiation of iPSCs to BMECs was verified using immunocytochemistry, as previously described.[26,27] Briefly, cells were fixed in either 100% ice-cold methanol or 4% paraformaldehyde, rinsed with PBS, and blocked for 30 min with either 10 or 40% goat serum (Sigma) in PBS. Particularly for P-glycoprotein and MRP1 immunolabeling, it is important to note that methanol-fixed cells are permeabilized during fixation. Cells were incubated with primary antibody diluted in 10% or 40% goat serum overnight at 4 °C, rinsed, and then incubated with goat anti-mouse or anti-rabbit Alexa Fluor 488 (1:200; Life Technologies) in 10 or 40% goat serum. Cell nuclei were counterstained with 4′,6-diamidino-2-phenylindole dihydrochloride (DAPI; Sigma). Primary antibodies used: PECAM-1 (Thermo Fisher, polyclonal, 1:25), Claudin-5 (Invitrogen, clone 4C3C2, 1:50), Occludin (Invitrogen, clone OC-3F10, 1:200), ZO-1 (Invitrogen, polyclonal, 1:100), VE-Cadherin (Santa Cruz Biotechnology, clone F-8, 1:25), BCRP (Millipore, clone 5D3, 1:50), MRP1 (Millipore, clone QCRL-1, 1:25), and P-glycoprotein (Neomarkers, clone F4, 1:25). Mouse IgG (BD Biosciences, clone HOPC-1) was used as immunolabeling isotype control.

APC Analogue Permeability Studies. BMEC Transwell monolayer tightness was assessed by measuring transendothelial electrical resistance (TEER) using a chopstick electrode EVOM2 system (World Precision Instruments, Sarasota, FL), and high tightness (>1500 Ω-cm^2) verified prior to permeability experiments. EC medium was replaced with PM20 medium (50:50 DMEM:F12 + B27 supplement + 1% antibiotics + 20 ng/mL each of EGF and bFGF) and allowed to equilibrate with the monolayers for 60 min, and TEER measured again. APC analogues or control compounds ([^{14}C]-sucrose and [^{3}H]-diazepam) were then added to PM20 medium and allowed to diffuse across the monolayers for 2 h. At the end of the experiment, barrier integrity was assessed by TEER to verify no significant decrease for experimental duration. Control compounds [^{14}C]-sucrose and [^{3}H]-diazepam were diluted in PM20 medium at a dilution of 0.4 μCi/mL. For absolute permeability analyses, each APC analogue was diluted to 1 μM in PM20. For comparative analyses (i.e., temperature, polarity, and inhibitor experiments), the following APC analogue concentrations were used that optimized equipment and compound sensitivity and reprodu-

DOI: 10.1021/acs.molpharmaceut.6b00441
Mol. Pharmaceutics 2016, 13, 3341−3349

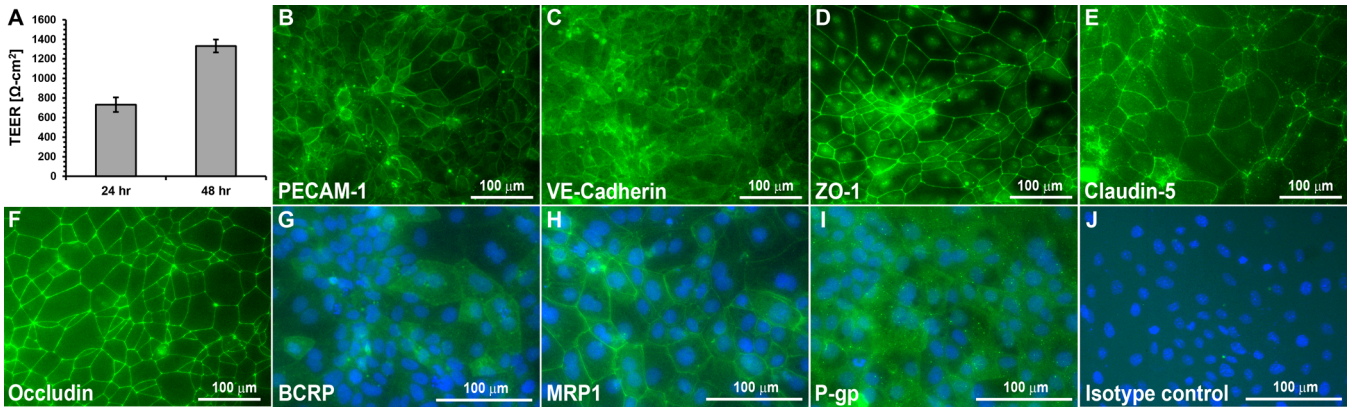

Figure 2. Characteristics of iPSC-derived BMECs. (A) iPSC-derived BMECs exhibit barrier tightening from 24 to 48 h as measured by TEER. Shown are data for a single iPSC differentiation to BMECs, $n = 3$ Transwell filters. Average 48 h TEER values across all experiments are denoted in the text. (B) iPSC-derived BMECs express BMEC proteins such as PECAM-1, (C) VE-Cadherin, (D) ZO-1, (E) Claudin-5, and (F) Occludin. iPSC-derived BMECs also express efflux transporters (G) BCRP, (H) MRP1, and (I) P-gp. (J) Isotype control antibody for efflux transporter immunostaining. In panels G–J, cell nuclei are labeled with DAPI (blue) to indicate the location of cells. Scale bar is 100 μm.

cibility: CLR1404 at 5–10 μCi/mL (average 0.3 μM), CLR1501 at 10 μg/mL (14 μM), and CLR1502 at 1 μg/mL (1.0 μM). At 30, 60, 90, and 120 min interval, an aliquot of 100 μL from the bottom chamber was collected and replaced by an equal volume of fresh PM20 medium. Fluorescence of CLR1501 and CLR1502 was assessed using a Safire II (Tecan Group Ltd., Männedorf, Switzerland). Radioactivity was measured using a TRICARB-PACKARD β-counter (PerkinElmer, Waltham, MA) or gamma counter (Wizard2 Automatic Gamma Counter, PerkinElmer, Waltham, MA). Permeability values were calculated as previously described.[34] Clearance volumes were plotted as a function of time, and linear regression was used to determine a clearance rate, denoted PSt for iPSC-derived BMEC coated filters and PSf for cell-free collagen-fibronectin coated filters. The PS value ascribed to the BMEC monolayer denoted PSe was subsequently calculated using $1/PSe = (1/PSf) - (1/PSt)$. Finally, the permeability, Pe (cm/min), was calculated by dividing by the surface area, S, of the filter, $Pe = PSe/S$.

Inhibition Studies. Pharmacological inhibition experiments were carried out by preincubating BMEC monolayers for 60 min with 1 μM PSC833 (P-gp inhibitor), 1 μM Ko143 (BCRP inhibitor), or 10 μM MK571 (pan-MRP inhibitor) in EC medium. Inhibition was maintained during the permeability experiments by adding these inhibitors at the same concentration in the PM20 medium. Otherwise permeability experiments were performed exactly as described above.

Statistical Analysis. All data in this study were expressed as mean ± SEM of at least three independent experiments. For comparison of two groups, a two-tailed unpaired Student's t test was used. With multiple experimental groups, a normal data distribution was verified and then analysis of variance (ANOVA) performed to determine statistical differences. Post hoc comparisons were performed upon ANOVA significance to look for specific differences between groups: Tukey test if equal sample sizes and similar population variance or Games–Howell if unequal sample sizes and high population variance.[35] Statistical significance was defined as $p < 0.05$. Statistics were determined using SPSS (version 22, IBM, Armonk, New York).

RESULTS

iPSC-Derived BMECs. Following our established protocols,[26,27] BMECs were differentiated from iPSCs (Figure 2). Differentiated BMECs exhibited high barrier properties that increased to a maximum 48 h after seeding onto Transwell inserts as measured by TEER (1500 ± 85 Ω-cm^2, Figure 2A). As previously described, iPSC-derived BMECs expressed endothelial proteins including PECAM-1 and VE-Cadherin. In addition, they expressed BBB tight junction proteins ZO-1, Claudin-5, and Occludin, and BBB efflux transporters including BCRP, MRP1, and P-gp (Figure 2B–J). APC analogue permeability studies were performed using these iPSC-derived BMECs.

Biophysical Characterization and BMEC Permeability of APC Analogues. The APC analogues CLR1404, CLR1501, and CLR1502 (Figure 1A) were first characterized for octanol:water partition coefficients (logD, pH7.4) and BBB-BMEC diffusion properties. Since it is highly lipophilic and not an efflux transport substrate, diazepam was used as a highly BBB-permeable control. Conversely, sucrose was used as a BBB-impermeable control because of its hydrophilicity and lack of brain-specific uptake mechanism.[26,32] All APC analogues exhibited high lipophilicity demonstrated by positive calculated logD (cLogD) and experimentally determined LogD values (Figure 1B). Notably, fluorescently tagged APC analogues CLR1501 and CLR1502 demonstrated greater than 2-fold increased LogD values compared to parent CLR1404 in experimentally determined samples.

Next, the permeability of APC analogues across the iPSC-derived in vitro BBB was analyzed using a Transwell system[26,27] (Figure 1C) and compared to diazepam and sucrose permeabilities.[26,32] All APC analogues demonstrated intermediate permeability across BBB-BMECs, with values substantially lower than that of diazepam but still 2–4-fold higher than that of impermeable sucrose (CLR1404:35 ± 5.7; CLR1501:54 ± 3.2; CLR1502:26 ± 4.9; diazepam, 170 ± 29; sucrose, 13 ± 2.5; all values expressed as $\times 10^{-5}$ cm/min, $p < 0.05$) (Figure 1D). In addition, CLR1404 and CLR1501 are of similar molecular weight and have similar intermediate permeability despite substantial differences in lipophilicity. CLR1501 and CLR1502 have the same high lipophilicity with CLR1502 having a higher molecular weight, and a 2-fold reduced permeability ($p < 0.05$) (Figure 1D). These initial APC analogue experiments suggested more complex permeability mechanisms than just simple diffusion, and therefore analysis of

DOI: 10.1021/acs.molpharmaceut.6b00441
Mol. Pharmaceutics 2016, 13, 3341–3349

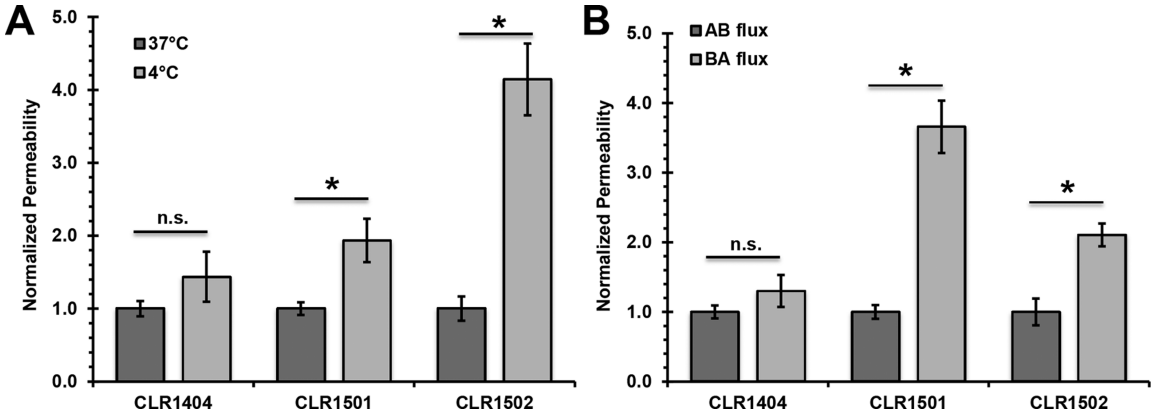

Figure 3. Examination of temperature and directional dependence of APC analogue permeability. (A) CLR permeability was determined at 4 and 37 °C. Permeability values were independently normalized to the 37 °C condition for each analogue (mean ± SE, $n \geq 3$ independent BMEC differentiation replicates, *$p < 0.05$ or n.s. = not significant compared to 37 °C by Student's t test). (B) Basolateral to apical (BA) and apical to basolateral (AB) permeabilities were measured and independently normalized to the AB permeability for each analogue (mean ± SE, $n \geq 3$ independent BMEC differentiation replicates, *$p < 0.05$ or n.s. = not significant compared to AB flux by Student's t test).

active cellular processes mediated by efflux transporters was undertaken.

Regulation of APC Analogue Permeability by Active Cellular Mechanisms. Next, the role of active mechanisms in regulating BBB penetration by APC analogues was examined. First, the impact of temperature was examined to determine the possible effects of active cellular uptake and/or efflux[36−38] (Figure 3A). A shift to 4 °C to curtail active uptake and efflux mechanisms resulted in a slight, but statistically insignificant, increase in BBB permeability for the parent APC analogue CLR1404, suggesting that its BBB permeability is largely driven by diffusive mechanisms. Conversely, CLR1501 and CLR1502 fluorescent APC analogues demonstrated significantly higher in vitro BBB permeability at 4 °C compared to cells incubated at 37 °C (Figure 3A, $p < 0.05$), suggesting a significant role for active efflux.

If active efflux plays a role, one would also expect a polarized permeability profile. Thus, the basolateral−apical (BA) and apical−basolateral (AB) APC analogue fluxes were compared to evaluate contributions of efflux mechanisms (Figures 1C and 3B). CLR1404 showed no significant evidence of polarized efflux demonstrated by influx (AB) compared to efflux (BA). In agreement with the temperature-dependent permeability profiles, CLR1501 and CLR1502 displayed an active efflux mechanism demonstrated by significantly polarized flux in the brain-to-blood (BA) direction (Figure 3B, $p < 0.05$). Taken together, the temperature dependence and polarized flux experiments demonstrated active cellular efflux mechanisms for CLR1501 and CLR1502, whereas CLR1404 is largely governed by diffusive mechanisms.

Efflux Transporter Substrate Profiles of APC Analogues. Given the putative efflux profiles for CLR1501 and CLR1502, we evaluated the potential involvement of the BBB drug efflux transporters breast cancer resistance protein (BCRP), multidrug resistance proteins (MRPs), and P-glycoprotein (P-gp) that are expressed in the iPSC-derived BMEC model (Figures 2G−2I). As previously described, efflux transporter activity in the iPSC-derived BMECs can be examined by employing specific pharmacological inhibitors Ko143, MK571, and PSC833 to inhibit BCRP, MRPs, and P-gp, respectively (Figure 4A).[26,27] Consistent with the results in Figure 3 regarding the apparent lack of active cellular mechanisms regulating CLR1404 permeability, the inhibition of drug efflux pumps did not affect observed CLR1404 permeability with statistical significance (Figure 4B). In contrast, CLR1501 permeability was selectively increased following treatment with Ko143 or MK571, suggesting the contribution of BCRP and MRPs in CLR1501 efflux (Figure 4C, $p < 0.05$). A similar pattern was observed for CLR1502, suggesting the contribution of both BCRP and MRP efflux (Figure 4D, $p < 0.05$). Substantial P-gp efflux was not detected since inhibition by PSC833 did not result in a statistically significant permeability change for any of the APC analogues.

Since efflux transporter mediated differences in BBB transport were observed only for the fluorescent APC analogues, the efflux profiles of unconjugated BODIPY and IR775 dyes alone were investigated. No significant change in BODIPY diffusion was measured with efflux transporter inhibition (Figure 4E), while IR-775 dye diffusion was only dependent on BCRP inhibition (Figure 4F, $p < 0.05$). Overall, these data suggest that, even though dye conjugation with APC analogues affects BBB permeability properties, cellular efflux is not completely dictated by the fluorescent dye moiety alone.

■ DISCUSSION

Through extensive structure−activity relationship studies of chemically synthesized PLE and APC derivatives, our group has identified cancer-targeting APC analogues that demonstrate tumor-selective uptake and prolonged retention in many cancer cell lines, in preclinical models, and in human cancer patients.[17,25,39,40] Of particular interest, there is a large unmet clinical need for efficacious treatments against malignant brain tumors, which exhibit high mortality and morbidity with poor overall survival.[3,41] Our versatile APC analogues could potentially be applied to improve brain tumor patient outcomes in multimodality clinical management such as diagnostic imaging, surgical staging, and planning using positron emission tomography (PET),[17] intraoperative tumor cell visualization using fluorescence,[18] and cytotoxic tumor therapy using cancer cell targeted radiation.[17,39] Our APC analogues have demonstrated a high tumor to normal brain ratio in initial clinical trials;[17] however, their blood−brain barrier permeability has not been characterized. Such knowledge can help guide development of APC analogues for clinical applications. For instance, gliomas often invade from the "leaky" tumor center

DOI: 10.1021/acs.molpharmaceut.6b00441
Mol. Pharmaceutics 2016, 13, 3341−3349

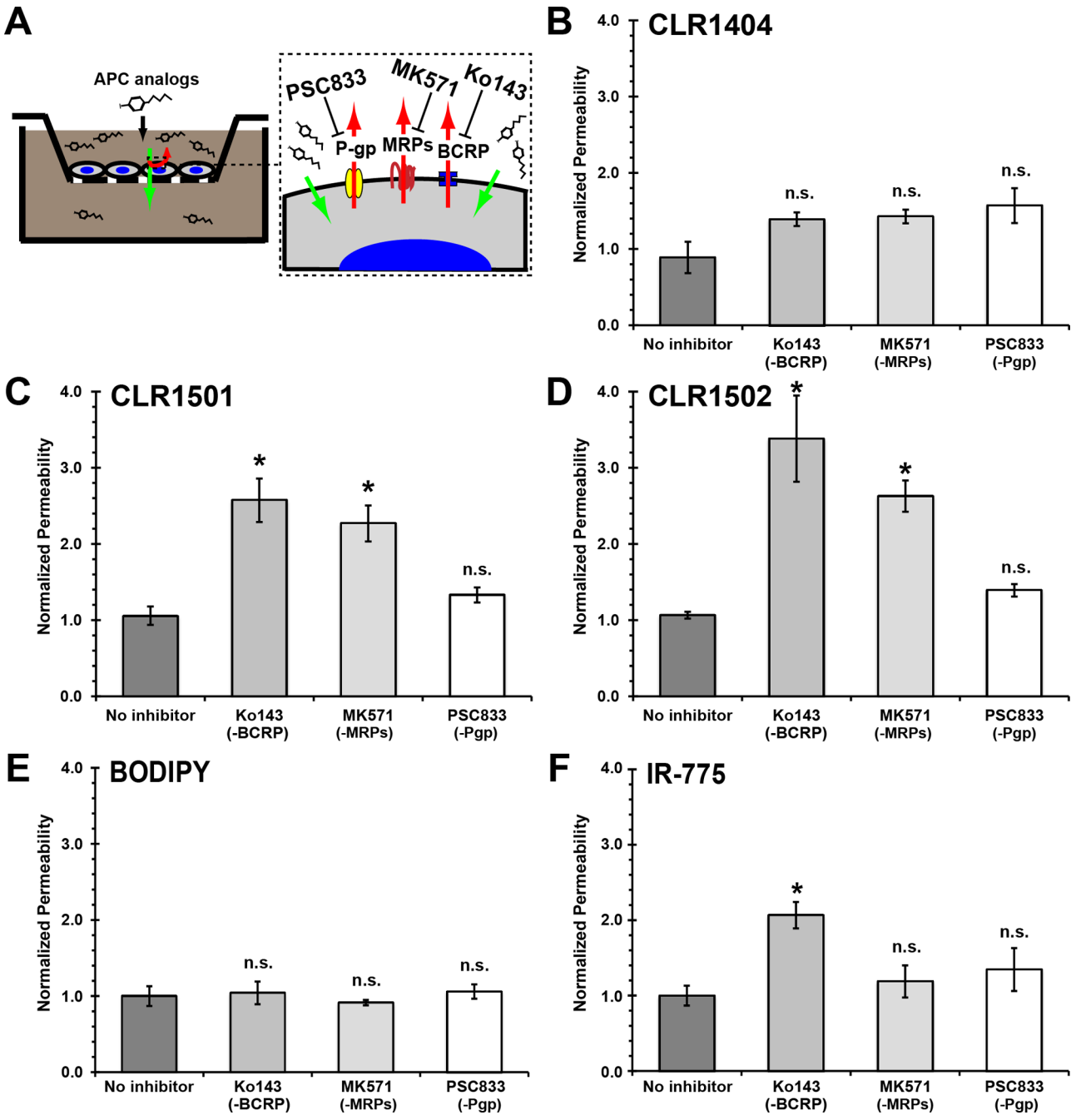

Figure 4. APC analogue permeability dependence on efflux transporters as demonstrated by BBB Transwell system using pharmacologic inhibitors. (A) Schematic of experimental setup. In the presence of inhibitors, one would expect an increase in permeability if targeted efflux transporter is involved: Ko143 inhibits BCRP, MK571 inhibits MRPs, and PSC833 inhibits P-gp. (B) Parent CLR1404, (C) CLR1501, (D) CLR1502, (E) free BODIPY, (F) free IR-775. All permeability values were normalized to the respective no inhibitor, vehicle controls (mean ± SE, $n \geq 3$ independent BMEC differentiation replicates, $^*p < 0.05$ or n.s. = not significant compared to no inhibitor by ANOVA followed by post hoc Games−Howell).

into normal brain with an intact BBB,[13] and therefore it may be possible that the high tumor-to-brain ratio is a result of BBB leakage into the tumor center, but infiltrating tumor cells may be inaccessible to standard intravenously delivered APC analogues. In this study with a human induced pluripotent stem cell (iPSC) BBB model,[26,27] we found that BBB permeability of APC analogues CLR1404, CLR1501 (green fluorescent), and CLR1502 (near-infrared) was modestly higher than permeability of sucrose, but despite their high lipophilicity, they had relatively low permeability compared with diazepam. Thus, we hypothesize that the high tumor-to-brain ratio observed clinically may partially result from BBB restriction of APC permeability in normal brain, compared to high APC permeability across disrupted tumor vasculature.

The APC backbone of CLR1404 can be highly modified with multiple moieties while retaining its tumor-targeting properties. To address how these modifications may affect BBB permeability, the biophysical properties of the different APC analogues were analyzed. Increased lipophilicity is a key determinant for enhanced BBB permeability,[42−45] and there is an inverse relationship between molecular weight and BBB permeability.[42,45] All CLR compounds are greater than 600 Da,

DOI: 10.1021/acs.molpharmaceut.6b00441
Mol. Pharmaceutics 2016, 13, 3341−3349

and thus above the typical molecular weight cutoff range (400–600 Da[45]) where BBB permeability and lipophilicity/molecular weight are most well correlated. Nonetheless, CLR1404 behaves generally as expected with a substantially lower permeability than diazepam as a function of its lowered lipophilicity and its modest increase in size. However, CLR1501 had a similar permeability to CLR1404 despite its similar molecular weight and much greater lipophilicity. In addition, CLR1502 had a very high lipophilicity and it is unlikely that its increase in molecular weight alone compared with CLR1404 can account for its relatively low permeability.[45] The permeability data therefore suggested that BMEC efflux transporters could significantly affect the transport of CLR1501 and CLR1502. Indeed, while the parent CLR1404 seemed comparatively unaffected by active efflux, both fluorescent analogues were significantly effluxed by BCRP and MRP efflux transporter systems. Therefore, while CLR1404 BBB permeability appears to be largely governed by passive diffusion, CLR1501 and CLR1502 are additionally regulated by efflux, and the net result is relatively similar in vitro BBB permeability among the analogues. Finally, even upon efflux transporter blockade, CLR1501 and CLR1502 had permeabilities that did not exceed diazepam despite their significantly higher lipophilicity. It is likely that, compared with diazepam, the higher molecular weights of CLR1501 and CLR1502 or their differential interactions with the lipid bilayer are contributing to their attenuated permeability properties. Previous work with the iPSC-derived BMEC model showed a good correlation between in vivo and in vitro permeability including for lipophilic efflux transporter substrates such as prazosin, colchicine, and vincristine.[26] However, the relative expression levels of the efflux transporters in any in vitro BBB model can vary compared with in vivo expression levels;[46,47] and hence, the absolute permeability values reported here will likely differ in vivo. Finally, P-gp did not play a significant role in efflux of our APC analogues in these analyses. However, the BCRP, MRP, and P-gp efflux transporters have overlapping substrate specificity and can potentially compensate for each other,[5,7,8] and future studies would be helpful in determining if P-gp contributes to APC analogue efflux upon reduced BCRP and/or MRP activity in transporter knockout animals.[48,49]

Parameters governing BBB permeability of small molecules can be complex,[42] particularly when combining multiple agents for multimodal cancer approaches (e.g., targeting and visualization).[6,50] As an independent entity, the chemical linkage itself may also affect BBB permeability.[50] Linker effects on CLR1501 and CLR1502 are unlikely, as moieties are directly linked to the phenyl ring (Figure 1) with no intermediate chemical groups. However, addition of the fluorescent moieties to the phenyl ring in CLR1501 (BODIPY) and CLR1502 (IR-775) clearly introduced efflux transporter recognition by BCRP and MRP. Neither free dye was determined to be as strong a substrate for efflux as the conjugated CLR1501 and CLR1502 molecules, even though IR-775 was effluxed to some extent by BCRP. It is possible that steric effects are introduced that explain efflux differences between free dyes and their respective APC analogues. Molecular size[5] and topological polar surface area[42,51] have been described as critical parameters to predict compounds as a substrate for P-gp, and therefore addition of the fluorescent moieties may change the substrate preferences of efflux transporters compared to the properties of parent CLR1404 or free dyes. Finally, drug solubility of the highly lipophilic APC analogues or differential molecular interactions with the BBB could lead to differences in analogue permeability. These and other considerations may aid in design and development of future generations of APC analogues for specific application in CNS disease. Ultimately, screening with a robust biological assay will likely be beneficial since properties governing BBB penetrance of small molecules have not been completely resolved.[42] The human iPSC-derived BMEC system employed here could be a powerful tool in this respect, as demonstrated for this first set of APC analogues.

In conclusion, we have characterized the blood–brain barrier permeability characteristics of novel cancer-targeting APC analogues using a human iPSC-derived BMEC model. Limited diffusion across the intact BBB helps explain initial clinical results in brain tumors that demonstrated very high tumor to normal brain ratios,[17] although additional preclinical and clinical analyses are needed to augment the findings of this study with respect to patient-specific APC analogue permeability and efflux. For clinical applications where greater brain penetration is advantageous, results of this study could aid in designing future APC analogues or help devise novel combination strategies such as administration of APC analogues with BCRP or MRP inhibitors. This study may also aid in the successful clinical translation of other fluorescent agents under development for CNS disorders and brain tumors.[52−54]

AUTHOR INFORMATION

Corresponding Authors

*Tel: (608) 262-7303. E-mail: kuo@neurosurgery.wisc.edu.
*Tel: (608) 265-5103. E-mail: eshusta@wisc.edu.

Author Contributions

P.A.C., A.J.A.-A., J.S.K., and E.V.S. designed the study and analyzed results. P.A.C., A.J.A.-A., T.Q., R.R.Z., and H.K.W. performed experiments within this study. J.P.W. and S.P.P. helped in experimental design and analysis. The manuscript was written through contributions of all authors. All authors have given approval to the final version of the manuscript. P.A.C. and A.J.A.-A. contributed equally to this work. J.S.K. and E.V.S. are co-corresponding authors.

Notes

The authors declare the following competing financial interest(s): Jamey P. Weichert is the founder and shareholder in Cellectar Biosciences that provided the APC analogues used in this study.

ACKNOWLEDGMENTS

Cellectar Biosciences (Madison, WI) kindly provided the APC analogues used in these studies. This work was supported by the National Institutes of Health Grants AA020476 (E.V.S., J.S.K., and S.P.P.) and NS083688 (E.V.S. and S.P.P.) and the University of Wisconsin Institute for Clinical and Translational Research, NIH/NCATS UL1TR000427 (E.V.S. and J.S.K.). R.R.Z was supported by the University of Wisconsin MD/PhD program via T32 GM008692. J.S.K. was also supported in part by NIH Grants CA158800, NS75995, Headrush Brain Tumor Research Professorship, and the Roger Loff Memorial Fund for GBM Research.

ABBREVIATIONS USED

GBM, glioblastoma multiforme; BBB, blood–brain barrier; APC, alkylphosphocholine; PSC, pluripotent stem cell; iPSC, induced PSC; BMEC, brain microvascular endothelial cell; P-

DOI: 10.1021/acs.molpharmaceut.6b00441
Mol. Pharmaceutics 2016, 13, 3341−3349

gp, P-glycoprotein; MRP, multidrug resistance protein; BCRP, breast cancer resistance protein; TEER, transendothelial electrical resistance; PLE, phospholipid ether

REFERENCES

(1) Ostrom, Q. T.; Gittleman, H.; Fulop, J.; Liu, M.; Blanda, R.; Kromer, C.; Wolinsky, Y.; Kruchko, C.; Barnholtz-Sloan, J. S. CBTRUS Statistical Report: Primary Brain and Central Nervous System Tumors Diagnosed in the United States in 2008−2012. *Neuro-Oncology* **2015**, *17* (Suppl. 4), iv1.

(2) American Cancer Society. *Cancer Facts and Figures 2015*; American Cancer Society: Atlanta, 2015.

(3) Stupp, R.; Mason, W. P.; van den Bent, M. J.; Weller, M.; Fisher, B.; Taphoorn, M. J.; Belanger, K.; Brandes, A. A.; Marosi, C.; Bogdahn, U.; Curschmann, J.; Janzer, R. C.; Ludwin, S. K.; Gorlia, T.; Allgeier, A.; Lacombe, D.; Cairncross, J. G.; Eisenhauer, E.; Mirimanoff, R. O. Radiotherapy plus concomitant and adjuvant Temozolomide for glioblastoma. *N. Engl. J. Med.* **2005**, *352* (10), 987−96.

(4) Puhalla, S.; Elmquist, W.; Freyer, D.; Kleinberg, L.; Adkins, C.; Lockman, P.; McGregor, J.; Muldoon, L.; Nesbit, G.; Peereboom, D.; Smith, Q.; Walker, S.; Neuwelt, E. Unsanctifying the sanctuary: challenges and opportunities with brain metastases. *Neuro-oncology* **2015**, *17* (5), 639−51.

(5) Schinkel, A. H. P-Glycoprotein, a gatekeeper in the blood−brain barrier. *Adv. Drug Delivery Rev.* **1999**, *36* (2−3), 179−194.

(6) Juillerat-Jeanneret, L. The targeted delivery of cancer drugs across the blood−brain barrier: chemical modifications of drugs or drug-nanoparticles? *Drug Discovery Today* **2008**, *13* (23−24), 1099−106.

(7) Borst, P.; Evers, R.; Kool, M.; Wijnholds, J. A family of drug transporters: the multidrug resistance-associated proteins. *Journal of the National Cancer Institute* **2000**, *92* (16), 1295−302.

(8) Loscher, W.; Potschka, H. Role of multidrug transporters in pharmacoresistance to antiepileptic drugs. *J. Pharmacol. Exp. Ther.* **2002**, *301* (1), 7−14.

(9) Warth, A.; Kroger, S.; Wolburg, H. Redistribution of aquaporin-4 in human glioblastoma correlates with loss of agrin immunoreactivity from brain capillary basal laminae. *Acta Neuropathol.* **2004**, *107*, 311−318.

(10) Bao, S.; Wu, Q.; Sathornsumetee, S.; Hao, Y.; Li, Z.; Hjelmeland, A. B.; Shi, Q.; McLendon, R. E.; Bigner, D. D.; Rich, J. N. Stem cell-like glioma cells promote tumor angiogenesis through vascular endothelial growth factor. *Cancer Res.* **2006**, *66*, 7843−8.

(11) Lockman, P. R.; Mittapalli, R. K.; Taskar, K. S.; Rudraraju, V.; Gril, B.; Bohn, K. A.; Adkins, C. E.; Roberts, A.; Thorsheim, H. R.; Gaasch, J. A.; Huang, S.; Palmieri, D.; Steeg, P. S.; Smith, Q. R. Heterogeneous blood-tumor barrier permeability determines drug efficacy in experimental brain metastases of breast cancer. *Clin. Cancer Res.* **2010**, *16* (23), 5664−78.

(12) Groothuis, D. R. The blood−brain and blood-tumor barriers: a review of strategies for increasing drug delivery. *Neuro-Oncology* **2000**, *2* (1), 45−59.

(13) Oberoi, R. K.; Parrish, K. E.; Sio, T. T.; Mittapalli, R. K.; Elmquist, W. F.; Sarkaria, J. N. Strategies to improve delivery of anticancer drugs across the blood−brain barrier to treat glioblastoma. *Neuro-oncology* **2016**, *18* (1), 27−36.

(14) Lockman, P. R.; Mittapalli, R. K.; Taskar, K. S.; Rudraraju, V.; Gril, B.; Bohn, K. A.; Adkins, C. E.; Roberts, A.; Thorsheim, H. R.; Gaasch, J. A.; Huang, S.; Palmieri, D.; Steeg, P. S.; Smith, Q. R. Heterogeneous blood-tumor barrier permeability determines drug efficacy in experimental brain metastases of breast cancer. *Clin. Cancer Res.* **2010**, *16*, 5664−78.

(15) Woodworth, G. F.; Dunn, G. P.; Nance, E. A.; Hanes, J.; Brem, H. Emerging insights into barriers to effective brain tumor therapeutics. *Front. Oncol.* **2014**, *4*, 126.

(16) Adkins, C. E.; Mittapalli, R. K.; Manda, V. K.; Nounou, M. I.; Mohammad, A. S.; Terrell, T. B.; Bohn, K. A.; Yasemin, C.; Grothe, T. R.; Lockman, J. A.; Lockman, P. R. P-glycoprotein mediated efflux limits substrate and drug uptake in a preclinical brain metastases of breast cancer model. *Front. Pharmacol.* **2013**, *4*, 136.

(17) Weichert, J. P.; Clark, P. A.; Kandela, I. K.; Vaccaro, A. M.; Clarke, W.; Longino, M. A.; Pinchuk, A. N.; Farhoud, M.; Swanson, K. I.; Floberg, J. M.; Grudzinski, J.; Titz, B.; Traynor, A. M.; Chen, H. E.; Hall, L. T.; Pazoles, C. J.; Pickhardt, P. J.; Kuo, J. S. Alkylphosphocholine analogs for broad-spectrum cancer imaging and therapy. *Sci. Transl. Med.* **2014**, *6* (240), 240ra75.

(18) Swanson, K. I.; Clark, P. A.; Zhang, R. R.; Kandela, I. K.; Farhoud, M.; Weichert, J. P.; Kuo, J. S. Fluorescent cancer-selective alkylphosphocholine analogs for intraoperative glioma detection. *Neurosurgery* **2015**, *76* (2), 115−23 and discussion 123−4..

(19) Snyder, F.; Blank, M. L.; Morris, H. P. Occurrence and nature of O-alkyl and O-alk-I-enyl moieties of glycerol in lipids of Morris transplanted hepatomas and normal rat liver. *Biochim. Biophys. Acta, Lipids Lipid Metab.* **1969**, *176* (3), 502−10.

(20) Snyder, F.; Wood, R. Alkyl and alk-1-enyl ethers of glycerol in lipids from normal and neoplastic human tissues. *Cancer Res.* **1969**, *29* (1), 251−7.

(21) Soodsma, J. F.; Piantadosi, C.; Snyder, F. The biocleavage of alkyl glyceryl ethers in Morris hepatomas and other transplantable neoplasms. *Cancer research* **1970**, *30* (2), 309−11.

(22) Rampy, M. A.; Chou, T. S.; Pinchuk, A. N.; Skinner, R. W.; Gross, M. D.; Fisher, S.; Wahl, R.; Counsell, R. E. Synthesis and biological evaluation of radioiodinated phospholipid ether analogs. *Nucl. Med. Biol.* **1995**, *22* (4), 505−12.

(23) Meyer, K. L.; Schwendner, S. W.; Counsell, R. E. Potential tumor or organ-imaging agents. 30. Radioiodinated phospholipid ethers. *J. Med. Chem.* **1989**, *32* (9), 2142−7.

(24) Rampy, M. A.; Brown, R. S.; Pinchuk, A. N.; Weichert, J. P.; Skinner, R. W.; Fisher, S. J.; Wahl, R. L.; Gross, M. D.; Ethier, S. P.; Counsell, R. E. Biological disposition and imaging of a radioiodinated alkylphosphocholine in two rodent models of breast cancer. *J. Nucl. Med.* **1996**, *37* (9), 1540−5.

(25) Pinchuk, A. N.; Rampy, M. A.; Longino, M. A.; Skinner, R. W.; Gross, M. D.; Weichert, J. P.; Counsell, R. E. Synthesis and structure-activity relationship effects on the tumor avidity of radioiodinated phospholipid ether analogues. *J. Med. Chem.* **2006**, *49* (7), 2155−65.

(26) Lippmann, E. S.; Azarin, S. M.; Kay, J. E.; Nessler, R. A.; Wilson, H. K.; Al-Ahmad, A.; Palecek, S. P.; Shusta, E. V. Derivation of blood−brain barrier endothelial cells from human pluripotent stem cells. *Nat. Biotechnol.* **2012**, *30* (8), 783−91.

(27) Lippmann, E. S.; Al-Ahmad, A.; Azarin, S. M.; Palecek, S. P.; Shusta, E. V. A retinoic acid-enhanced, multicellular human blood−brain barrier model derived from stem cell sources. *Sci. Rep.* **2014**, *4*, 4160.

(28) Rampy, M. A.; Pinchuk, A. N.; Weichert, J. P.; Skinner, R. W.; Fisher, S. J.; Wahl, R. L.; Gross, M. D.; Counsell, R. E. Synthesis and biological evaluation of radioiodinated phospholipid ether stereoisomers. *J. Med. Chem.* **1995**, *38* (16), 3156−62.

(29) Glowka, F. K.; Romanski, M.; Siemiatkowska, A. Determination of partition coefficients n-octanol/water for treosulfan and its epoxy-transformers: an example of a negative correlation between lipophilicity of unionized compounds and their retention in reversed-phase chromatography. *J. Chromatogr. B: Anal. Technol. Biomed. Life Sci.* **2013**, *923−924*, 92−7.

(30) dos Reis, R. R.; Sampaio, S. C.; de Melo, E. B. An alternative approach for the use of water solubility of nonionic pesticides in the modeling of the soil sorption coefficients. *Water Res.* **2014**, *53*, 191−9.

(31) Leo, A.; Hansch, C.; Elkins, D. Partition Coefficients and Their Uses. *Chem. Rev.* **1971**, *71* (6), 525.

(32) Marchi, N.; Oby, E.; Batra, A.; Uva, L.; De Curtis, M.; Hernandez, N.; Van Boxel-Dezaire, A.; Najm, I.; Janigro, D. In vivo and in vitro effects of pilocarpine: relevance to ictogenesis. *Epilepsia* **2007**, *48* (10), 1934−46.

(33) Yu, J.; Vodyanik, M. A.; Smuga-Otto, K.; Antosiewicz-Bourget, J.; Frane, J. L.; Tian, S.; Nie, J.; Jonsdottir, G. A.; Ruotti, V.; Stewart, R.; Slukvin, II; Thomson, J. A. Induced pluripotent stem cell lines derived from human somatic cells. *Science* **2007**, *318* (5858), 1917−20.

DOI: 10.1021/acs.molpharmaceut.6b00441
Mol. Pharmaceutics 2016, 13, 3341−3349

(34) Perriere, N.; Demeuse, P.; Garcia, E.; Regina, A.; Debray, M.; Andreux, J. P.; Couvreur, P.; Scherrmann, J. M.; Temsamani, J.; Couraud, P. O.; Deli, M. A.; Roux, F. Puromycin-based purification of rat brain capillary endothelial cell cultures. Effect on the expression of blood–brain barrier-specific properties. *J. Neurochem.* **2005**, *93* (2), 279–89.
(35) Field, A. P. *Discovering statistics using IBM SPSS Statistics: and sex and drugs and rock 'n' roll*; 4th ed.; SAGE: London, 2013.
(36) Politi, P. M.; Arnold, S. T.; Felsted, R. L.; Sinha, B. K. P-glycoprotein-independent mechanism of resistance to VP-16 in multidrug-resistant tumor cell lines: pharmacokinetic and photoaffinity labeling studies. *Mol. Pharmacol.* **1990**, *37* (6), 790–6.
(37) Lin, J. T.; Sharma, R.; Grady, J. J.; Awasthi, S. A flow cell assay for evaluation of whole cell drug efflux kinetics: analysis of paclitaxel efflux in CCRF-CEM leukemia cells overexpressing P-glycoprotein. *Drug Metab. Dispos.* **2001**, *29* (2), 103–10.
(38) Hidalgo, I. J.; Borchardt, R. T. Transport of a large neutral amino acid (phenylalanine) in a human intestinal epithelial cell line: Caco-2. *Biochim. Biophys. Acta, Biomembr.* **1990**, *1028* (1), 25–30.
(39) Grudzinski, J. J.; Titz, B.; Kozak, K.; Clarke, W.; Allen, E.; Trembath, L.; Stabin, M.; Marshall, J.; Cho, S. Y.; Wong, T. Z.; Mortimer, J.; Weichert, J. P. A phase 1 study of 131I-CLR1404 in patients with relapsed or refractory advanced solid tumors: dosimetry, biodistribution, pharmacokinetics, and safety. *PLoS One* **2014**, *9* (11), e111652.
(40) Deming, D. A.; Maher, M. E.; Leystra, A. A.; Grudzinski, J. P.; Clipson, L.; Albrecht, D. M.; Washington, M. K.; Matkowskyj, K. A.; Hall, L. T.; Lubner, S. J.; Weichert, J. P.; Halberg, R. B. Phospholipid ether analogs for the detection of colorectal tumors. *PLoS One* **2014**, *9* (10), e109668.
(41) Ostrom, Q. T.; Bauchet, L.; Davis, F. G.; Deltour, I.; Fisher, J. L.; Langer, C. E.; Pekmezci, M.; Schwartzbaum, J. A.; Turner, M. C.; Walsh, K. M.; Wrensch, M. R.; Barnholtz-Sloan, J. S. The epidemiology of glioma in adults: a "state of the science" review. *Neuro-oncology* **2014**, *16* (7), 896–913.
(42) Rankovic, Z. CNS drug design: balancing physicochemical properties for optimal brain exposure. *J. Med. Chem.* **2015**, *58* (6), 2584–608.
(43) Hansch, C.; Steward, A. R.; Anderson, S. M.; Bentley, D. The parabolic dependence of drug action upon lipophilic character as revealed by a study of hypnotics. *J. Med. Chem.* **1968**, *11* (1), 1–11.
(44) Upadhyay, R. K. Drug delivery systems, CNS protection, and the blood brain barrier. *BioMed Res. Int.* **2014**, *2014*, 869269.
(45) Levin, V. A. Relationship of octanol/water partition coefficient and molecular weight to rat brain capillary permeability. *J. Med. Chem.* **1980**, *23* (6), 682–4.
(46) Uchida, Y.; Ohtsuki, S.; Katsukura, Y.; Ikeda, C.; Suzuki, T.; Kamiie, J.; Terasaki, T. Quantitative targeted absolute proteomics of human blood–brain barrier transporters and receptors. *J. Neurochem.* **2011**, *117* (2), 333–45.
(47) Ohtsuki, S.; Ikeda, C.; Uchida, Y.; Sakamoto, Y.; Miller, F.; Glacial, F.; Decleves, X.; Scherrmann, J. M.; Couraud, P. O.; Kubo, Y.; Tachikawa, M.; Terasaki, T. Quantitative targeted absolute proteomic analysis of transporters, receptors and junction proteins for validation of human cerebral microvascular endothelial cell line hCMEC/D3 as a human blood–brain barrier model. *Mol. Pharmaceutics* **2013**, *10* (1), 289–96.
(48) Oberoi, R. K.; Mittapalli, R. K.; Elmquist, W. F. Pharmacokinetic assessment of efflux transport in sunitinib distribution to the brain. *J. Pharmacol. Exp. Ther.* **2013**, *347* (3), 755–64.
(49) Agarwal, S.; Elmquist, W. F. Insight into the cooperation of P-glycoprotein (ABCB1) and breast cancer resistance protein (ABCG2) at the blood–brain barrier: a case study examining sorafenib efflux clearance. *Mol. Pharmaceutics* **2012**, *9* (3), 678–84.
(50) Misra, A.; Ganesh, S.; Shahiwala, A.; Shah, S. P. Drug delivery to the central nervous system: a review. *J. Pharm. Pharm. Sci.* **2003**, *6* (2), 252–73.
(51) Desai, P. V.; Sawada, G. A.; Watson, I. A.; Raub, T. J. Integration of in silico and in vitro tools for scaffold optimization during drug discovery: predicting P-glycoprotein efflux. *Mol. Pharmaceutics* **2013**, *10* (4), 1249–61.
(52) Stummer, W.; Reulen, H. J.; Novotny, A.; Steppe, H.; Tonn, J. C. Fluorescence-guided resections of malignant gliomas–an overview. *Acta Neurochir. Suppl.* **2003**, *88*, 9–12.
(53) Liu, J. T.; Meza, D.; Sanai, N. Trends in fluorescence image-guided surgery for gliomas. *Neurosurgery* **2014**, *75* (1), 61–71.
(54) Butte, P. V.; Mamelak, A.; Parrish-Novak, J.; Drazin, D.; Shweikeh, F.; Gangalum, P. R.; Chesnokova, A.; Ljubimova, J. Y.; Black, K. Near-infrared imaging of brain tumors using the Tumor Paint BLZ-100 to achieve near-complete resection of brain tumors. *Neurosurgical focus* **2014**, *36* (2), E1.

DOI: 10.1021/acs.molpharmaceut.6b00441
Mol. Pharmaceutics 2016, 13, 3341–3349